

SPECTRODIRECTIONAL FIELD AND LABORATORY MEASUREMENTS OF AN ARTIFICIAL TARGET

Jürg T. Schopfer, Stefan Dangel, Tanya Rodriguez, Mathias Kneubühler and Klaus Itten

University of Zurich, Department of Geography, Remote Sensing Laboratories RSL, Zurich, Switzerland; jschopfer@geo.unizh.ch

ABSTRACT

Spectrodirectional experiments with goniometer systems are only able to observe approximations of truly directional surface reflectance properties (BRDF). The directly observed quantity in field experiments is called hemispherical directional reflectance factor (HDRF), corresponding to hemispherical illumination, which depends on the atmospheric conditions, and directional observation. Laboratory experiments suffer from imperfect illumination resulting in a biconical rather than bidirectional reflectance factor. Quantitative comparison of field and laboratory measurements is not only important to ensure effective comparability, but also to permit cross-calibration of the experimental devices and to document the degree of compatibility. It is further a prerequisite for determining for which targets a replacement of field by laboratory experiments is feasible. Preliminary studies (i) revealed that the diffuse illumination present in the field is one of the major differences between field and laboratory measurements.

A goal of this study is to characterize and correct the diffuse influence in spectrodirectional field measurements more accurately and validate previously achieved results. Spectrodirectional field measurements were accomplished using a GER3700 spectroradiometer mounted on the field goniometer system (FIGOS) of the Remote Sensing Laboratories (RSL, Switzerland). Additionally, an MFR and a REAGAN sun photometer were permanently monitoring the atmospheric conditions. The laboratory goniometer system (LAGOS) uses a 1000W brightness-stabilized quartz tungsten halogen lamp as illumination source. For both field and laboratory measurements, we used an inert and highly anisotropic target. Field data were corrected for diffuse illumination following a procedure proposed by Martonchik (ii). The diffuse influence is then computed as a correction term depending on the angular characteristic of the target BRDF and of the amount of diffuse irradiance. Additionally, the diffuse sky radiance distribution is simulated through multiple runs of MODTRAN (iii) and will be implemented within the correction algorithm in further studies.

INTRODUCTION

The goniometer system of the Remote Sensing Laboratory (RSL) can be used for spectrodirectional field measurements (Field Goniometer System FIGOS) and spectrodirectional laboratory measurements (Laboratory Goniometer System LAGOS). However, there are obvious differences between the two cases, which have to be considered:

- In field experiments the target is left in its natural environment and is exposed to the natural direct and diffuse illumination. Diffuse illumination is depending on the illumination zenith angle and the atmospheric conditions. It is present in the field also under clear sky conditions, but is usually neglected in the laboratory.
- The direct illumination by the sun can be treated as being parallel (within 0.5°) and homogeneous over the area and height profile of the target, while laboratory illumination is usually non-parallel, non-homogeneous and not constant as a function of the target height.
- The illuminated area in the laboratory is limited; adjacency and multiple scattering effects can therefore be very different to field experiments.

- The spectrum of artificial light sources differs from that of the sun, which is additionally attenuated by the atmosphere. This is usually neglected since reflectance measurements are normalized using a reference target.
- The polarization of the natural and artificial light sources can be different.
- Living plants may behave differently under field and laboratory conditions.

Taking these differences into account, the advantage of laboratory measurements lies in the independence of weather conditions, time of day or seasonal conditions. The illumination intensity and angles can be held constant over time and freely chosen.

Currently, there exists only one systematic comparison of field and laboratory measurements using the same artificial target (1). This study has been performed as a consequence and focuses on an improvement of the obtained correction results by allowing for various noticed drawbacks such as the target size, the reference height and rotational symmetry of the target.

The directional surface reflectance properties are by definition characterized by the bidirectional reflectance distribution function (BRDF), or equivalently, the bidirectional reflectance factor (BRF) and depend on the surface properties only. However, spectrodirectional field experiments with goniometer systems are only able to observe approximations of the bidirectional reflectance factor. The directly observed quantity in field experiments is called hemispherical conical reflectance factor (HCRF), corresponding to hemispherical illumination, which depends on the atmospheric conditions, and conical observation. Laboratory experiments suffer from imperfect illumination resulting in a rather biconical than bidirectional reflectance factor. In this study the conicality on the illumination and observation side has been neglected. This is acceptable for the observation side since the field of view (FOV) of the sensor is quite small (3°). Current studies at RSL pay attention to the conicality of both the illumination source and the sensor. Additionally, the changing size and position of the sensor's footprint as a function of the observation angle have to be considered, especially if the target is not very large or exhibits different BRDF's at different parts.

In order to make measurement results of field and laboratory spectrodirectional experiments directly comparable, we need to retrieve the BRDF for both cases. For the field case we followed the well known procedures proposed by Martonchik and others (2) (iv), which correct the measurements only for the diffuse illumination and not for any other imperfections. For these methods, the diffuse radiation has to be measured over the complete hemisphere at the same angular resolution as the reflected radiation of the target. Since we are not yet able to measure the incoming diffuse radiation at angular resolution, we used a simplified approach measuring the diffuse irradiance with an MFR sun photometer. Additionally, a tool was developed which consolidates multiple MODTRAN runs in order to describe the diffuse sky radiance distribution. For the laboratory case, the approximated BRF is used since the standard retrieval schemes do not apply because they rely on the separation of direct and diffuse illumination.

METHODS

Comparison requirements

For comparison purposes of spectrodirectional field and laboratory measurements it is necessary to hold as many parameters as possible constant. So, the target, the measurement instruments, the experiment setup, the illumination and observation geometries, directions and areas remain the same. As mentioned, a basic difference of the two measurement cases is that in the laboratory we obtain BRF data and in the field HDRF data, using the approximations discussed above. Field data is influenced by atmospheric conditions, especially by the diffuse irradiance, which has to be corrected. For spectral analysis we compare the averaged nadir reflectances from 400 to 1200 nm. Directional analysis is mainly done in the solar principle plane at a wavelength of 496 nm.

- A) Target:** For the direct comparison of spectrodirectional field and laboratory measurements we used a new artificial, inert target, constructed at RSL (Fig.1) according to (v). The target size is 0.8 m x 0.8 m and it consists of a matrix of cubes, carved out of a thick plate of sanded duralumin. The spectrodirectional properties show a high angular anisotropy due to the cast shadows of the cubes as a function of the illumination angles. Furthermore, its BRDF is not rotationally symmetric (only 90° symmetry), it depends on the illumination and view azimuth angles. In order to reduce adjacency effects due to the limited size of the target, a black aluminum plate (size 1.2 m x 1.2 m) was used as background in both the laboratory and field case.

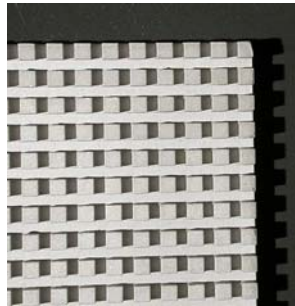


Fig. 1: Anisotropic target consisting of a matrix of cubes, carved out of a duralumin plate.

- B) Instruments and experiment setup:** The field and laboratory experiments were performed using the same measurement setup: a GER3700 sensor, mounted on the goniometer system, measuring the spectrodirectional reflectances over the whole hemisphere at an azimuthal angular resolution of 30° and a zenithal angular resolution of 15°. For a detailed description of RSL's goniometer system please refer to Sandmeier et al. (vi). In the field case, the total and diffuse illumination is permanently measured with an MFR-7 sun photometer (Yankee Environmental Systems Inc.) at 6 wavelengths (415, 500, 615, 673, 870, and 940 nm). The direct illumination is measured with a Reagan sun photometer (University of Arizona, Tucson USA) at 10 wavelengths (382, 410, 501, 611, 669, 721, 780, 872, 940 and 1033 nm). In the laboratory case, a 1000W brightness-stabilized quartz tungsten halogen lamp was used as illumination source (vii). The lamp is mounted on an adjustable tripod, which allows the use of the same illumination directions of the target as in the field case.
- C) Illuminated area:** The illumination distance (distance from the light source to the centre of the target) in the laboratory was held constant at 1.54 m for all illumination angles. However, for larger illumination zenith angles the semi-major axis of the ellipse is changing, which leads to an increase of the inhomogeneity and non-parallelism over the illuminated area. These effects were neglected in this study since the illumination distance remains the same and those effects particularly appear in the forward direction and at a great distance from the central part of the beam.
- D) Observed area:** Similar effects of a changing instantaneous ground field of view (IGFOV) also occur on the observation side. In order to reduce adjacency effects, large observation angles may be neglected in the analysis depending on A) and C).

Correction for diffuse irradiance

There are various methods to assess the diffuse illumination in HDRF measurements (2), (4). In this study we followed the procedure from Martonchik (2), where the incidence irradiance is split up into a direct and diffuse component $E_{dir}^{inc}(\mu_0)$ and $E_{diff}^{inc}(\mu_0)$. The diffuse influence then is accounted for in a correction term which is subtracted from the reflected field radiances $L(\mu, \mu_0, \varphi, \varphi_0)$. The resulting BRF_{Δ} then is

$$BRF_{\Delta} = \frac{L(\mu, \mu_0, \varphi, \varphi_0) - \Delta(\mu, \mu_0, \varphi, \varphi_0)}{\pi^{-1}[E_{dir}^{inc}(\mu_0) + E_{diff}^{inc}(\mu_0)]}, \quad (1)$$

where

μ, μ_0 is the cosine of the view and illumination zenith angle and

φ, φ_0 is the view and illumination azimuth angle.

$E_{dir}^{inc}(\mu_0)$ and $E_{diff}^{inc}(\mu_0)$ are measured by the MFR and the diffuse influence is described by

$$\Delta(\mu, \mu_0, \varphi, \varphi_0) = \pi^{-1} \int_0^1 \int_0^{2\pi} R(\mu, \mu', \varphi, \varphi') L_{diff}^{inc}(\mu', \mu_0, \varphi', \varphi_0) d\Omega - \pi^{-1} R(\mu, \mu_0, \varphi, \varphi_0) \int_0^1 \int_0^{2\pi} L_{diff}^{inc}(\mu', \mu_0, \varphi', \varphi_0) d\Omega, \quad (2)$$

where

R is the BRF of the target,

$L_{diff}^{inc}(\mu', \mu_0, \varphi', \varphi_0)$ is the diffuse incident radiance [$Wm^{-2}sr^{-1}$] and

$d\Omega$ is $\mu' d\mu' d\varphi'$, the projected solid angle.

In our case we assume that L_{diff}^{inc} is constant over the angles (since the MFR only observes the total incoming diffuse irradiance), and therefore the integral $\int_0^1 \int_0^{2\pi} L_{diff}^{inc}(\mu', \mu_0, \varphi', \varphi_0) d\Omega$ becomes the

constant factor $E_{diff}^{inc}(\mu_0)$:

$$\Delta \cong \pi^{-1} E_{diff}^{inc}(\mu_0) (\pi^{-1} \int_0^1 \int_0^{2\pi} R(\mu, \mu', \varphi, \varphi') d\Omega - R(\mu, \mu_0, \varphi, \varphi_0)), \quad (3)$$

The Δ -term in equation (3) is a function of the diffuse irradiance and the target anisotropy. The anisotropy is determined using the difference of the target BRF and the BRF integrated for a specific illumination angle.

Simulation of the diffuse sky radiance distribution

Correction results for the diffuse influence may be more accurate if the incoming diffuse radiation L_{diff}^{inc} is known at angular resolution, as pointed out in equation (2). Since we are not yet able to measure L_{diff}^{inc} the diffuse sky radiance distribution was simulated using MODTRAN (3). This is mainly done in two steps, an inversion and the subsequent forward modelling. As a result of the inversion, the values of the parameters O_3 , H_2O and visibility want to be known for the corresponding measurement time. Therefore a non-linear least square fit is computed between the measured vertical optical depth $\tau_{vert, Reagan}$ and the modelled vertical optical depth $\tau_{vert, MODTRAN}$. The obtained parameters for O_3 , H_2O and visibility, as well as the determined adequate aerosol model, then serve as an input to MODTRAN in order to simulate the diffuse light. A second routine has been developed for this purpose which allows the user to choose minimum and maximum sensor angles (zenith and azimuth) with adequate increments. For an overview of the simulation process please refer to Fig. 2:

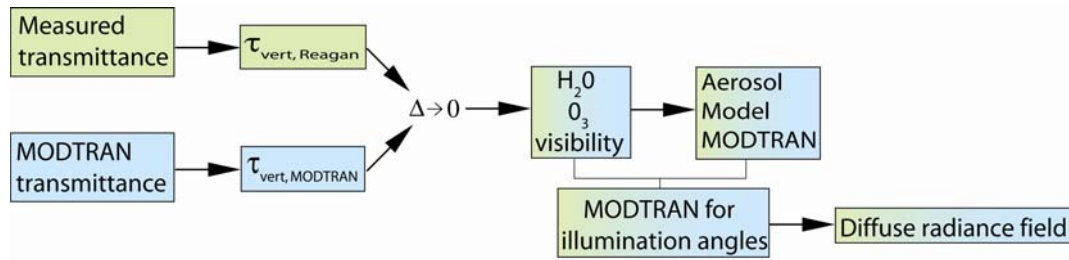


Fig. 2: Flowchart depicting the simulation for the sky radiance distribution

DATA

The field data for this study has been acquired in summer 2004 in Vordemwald (Switzerland). For the correction of the diffuse irradiance a similar (same instruments and measurement setup) dataset which was obtained in summer 2002 in Gilching (D), was used (1). With FIGOS, a total of 7 hemispheres of the artificial target were measured at different illumination zenith angles. The direct irradiance was permanently measured from 10:00h until 19:00h by a Reagan sun photometer (Fig. 3). Meteorological conditions were favourable with blue sky conditions for the whole measurement day.

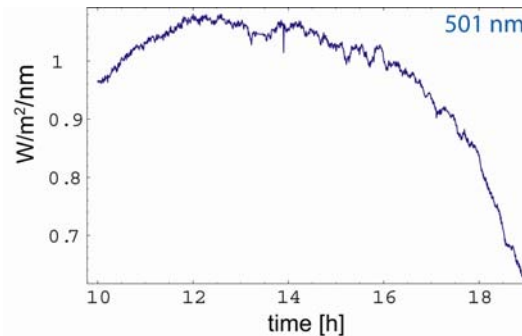


Fig. 3: Measured direct irradiance

The diffuse irradiance field was modelled using multiple runs of MODTRAN for corresponding illumination zenith angles and inverted atmospheric parameters (Fig. 2).

For LAGOS, 7 hemispheres under the same illumination angles as in the field have been measured in the goniometer laboratory at RSL. Table 1 shows an overview of the spectrodirectional dataset:

Table 1: Spectrodirectional dataset from FIGOS and LAGOS measurements

Hemisphere	Mean zenith zn [°]
Labhem/hem_a	29.6
Labhem/hem_b	28.8
Labhem/hem_c	31.7
Labhem/hem_d	39.8
Labhem/hem_e	48.1
Labhem/hem_f	58
Labhem/hem_g	68.1

RESULTS

Generally, the nadir reflectance over the whole spectrum is decreasing with an increasing illumination zenith angle. Nadir reflectances of FIGOS show higher values than of LAGOS. The extent of reflectance difference depends on the illumination zenith angle, shallow illumination produces large

shadowed areas which are illuminated by diffuse irradiance in the field, but not in the laboratory (Fig. 4):

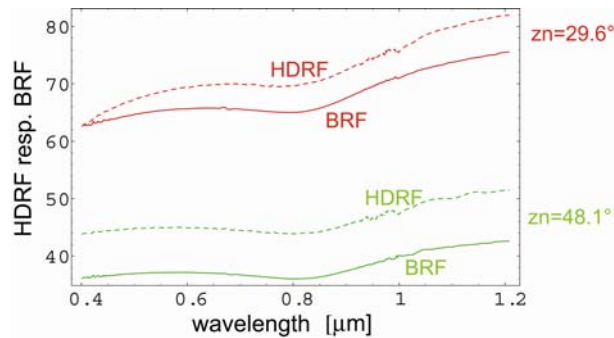


Fig. 4: Reflectance difference for nadir reflectances of labhem/hem_a and labhem/hem_e

Correction results and simulation of the diffuse sky radiance field

The correction is performed using $E_{diff}^{inc}(\mu_0)$ in equation (3). A comparison of the mean reflectances of the corrected BRF_{Δ} data to the original field and laboratory data reveals, that for large illumination zenith angles the correction is better than for small illumination zenith angles. However, the significance of the mean reflectance is minor, since only zenith angles from $+45^{\circ}$ to -45° are considered. The correction quality is therefore mainly discussed in the solar principal plane. The correction term is not useful for atmospherically little influenced hemispheres, since the diffuse influence is small and the correction method is not very sensitive.

The depicted hemispheres in Fig. 5 were measured at solar illumination zenith angles of 59.4° and 28.5° . The diffuse influence is present in both cases, either due to the large solar illumination zenith angle in a) or due to atmospheric conditions in b). However, the correction performance is very different as shown below (Fig. 5):

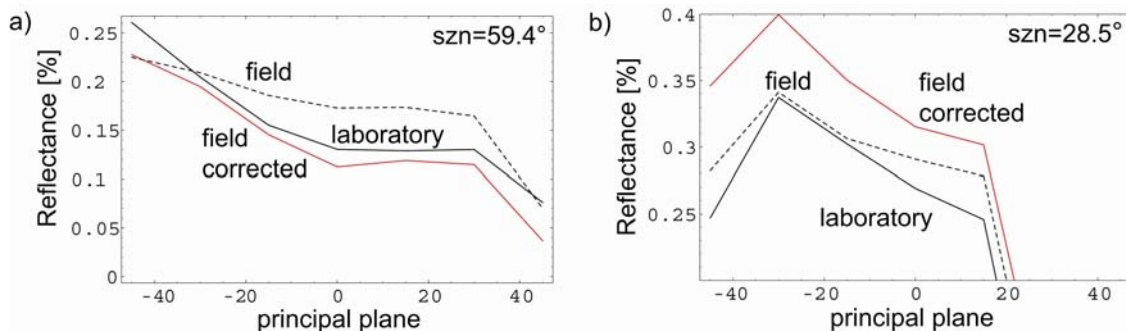


Fig 5: Correction for diffuse influence depending on its origin: a) illumination zenith angle, b) clouds

Diffuse irradiance due to the illumination angle is corrected quite good. However for other hemispheres which are also strongly influenced by diffuse irradiance, the correction term fails. An explanation might be, that the diffuse irradiance here is caused by moving clouds, instead of a large illumination zenith angle. This might lead to an inhomogeneous diffuse irradiance, which is not accounted for with our approximation for equation (3) (homogenous) for the incident diffuse radiance.

It is therefore necessary to know the distribution of the diffuse irradiance at angular resolution. First simulations of the diffuse sky radiance distribution show reasonable results as depicted in Fig. 6 for hem_a (mean zenith: 29.6° , time: 1300h LT). Meteorological conditions were favourable and the direct irradiance was dominant at the time of measurement, resulting in a little and symmetric influence of the diffuse irradiance along the principal plane. As expected, the diffuse influence is increasing with increasing illumination zenith angle.

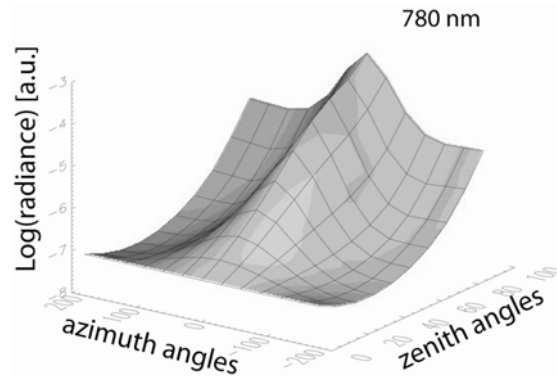


Fig. 6: Diffuse radiance field (displayed as log-plot) for hem_a at 1300h LT for 780 nm

Sufficient knowledge about the distribution of the diffuse sky radiance will provide the possibility to assess more accurately for the diffuse influence in spectrodirectional measurements, in particular for the inhomogeneous diffuse irradiance due to changing meteorological conditions.

CONCLUSION

In this study a direct comparison of spectrodirectional field and laboratory measurements using an artificial target has been performed. We concentrated on the difference due to the diffuse illumination and applied a correction method following the well known approach by Martonchik (2). For the comparison, an inert (no variation over time) and highly anisotropic (large Δ , stronger directional effects due to diffuse light), artificial target was chosen. Additionally, first simulations of the distribution of the diffuse sky radiance were performed. The conclusions of the obtained results are depicted as follows:

- The spectral analysis shows a higher nadir reflectance in field measurements than in the laboratory. This difference increases with increasing illumination zenith angle and occurs due to illumination of shadowed areas in the field case.
- The diffuse irradiance in field measurements leads to a levelling of dominant structures. Maximal reflectance values were obtained in the forward scattering region for an illumination zenith angle of 30° or larger.
- An assessment of the correction method seems difficult, since it is not sensitive enough for field measurements underlying only little diffuse influence. However, for field measurements with large illumination zenith angles good results were obtained. Obviously the angular distribution of the diffuse irradiance may differ depending on its origin, either caused by a long solar radiation path or by a changing atmosphere (sky cover).
- Simulations of the diffuse sky radiance distribution show reasonable results. Having this knowledge provides the possibility of performing more accurate corrections of the diffuse influence, in particular for an inhomogeneous distribution of the diffuse irradiance.

For future investigations concerning the influence of diffuse irradiance in spectrodirectional field measurements a large dataset with varying atmospheric conditions is necessary. Better correction can be obtained by measuring the incoming diffuse radiation at the same angular resolution and time as the spectrodirectional reflectance. To determine the potential and accuracy of such a correction the simulated diffuse sky radiance field will be implemented in the correction algorithm. Subsequent steps will then aim towards a goniometer system with two spectroradiometers, one looking upwards and one looking downwards.

For this comparison study approximations concerning illumination and observation geometries have been made for the laboratory case. Further research (viii) is currently done at RSL to account for the non-parallelism of the illumination and inhomogeneity of the illuminated area.

References

- i Schopfer J.T., S. Dangel, M. Kneubühler, G. Schaepman-Strub, M.E. Schaepman & K.I. Itten, 2004. Comparison of field and laboratory spectrodirectional measurements using an artificial target. In: SPIE Proceedings, 5570, 626-633
- ii Martonchik J.V. 1994. Retrieval of surface directional reflectance properties using ground level multiangle measurements. In: Remote Sensing of Environment, 303-316
- iii Berk A., G.P. Anderson, P.K. Acharya et al., 2003. MODTRAN4 Version 3 Revision 1 User's Manual, Air Force Research Laboratory, Hanscom AFB, MA 01731-3010
- iv Lyapustin A.I., J.L. Privette, 1999. A new method of retrieving surface bidirectional reflectance from ground measurements: Atmospheric sensitivity study. In: Journal of Geophysical Research, 104, 6257-6268
- v Govaerts Y., M. Verstraete & B. Hosgood, 1997. Evaluation of a 3-d radiative transfer model against goniometer measurements on an artificial target. In: Journal of Remote Sensing, 1, 131-136
- vi Sandmeier S.R. & K.I. Itten, 1999. A field goniometer system (FIGOS) for acquisition of hyperspectral BRDF data. In: IEEE Transactions on Geoscience and Remote Sensing, 37, 978-986
- vii Dangel S. et al., 2003. Combined field and laboratory goniometer system – FIGOS and LAGOS. In: International Geoscience and Remote Sensing Symposium IGARSS
- viii Dangel S., M.M. Verstraete, J.T. Schopfer, M. Kneubühler, M.E. Schaepman & K.I. Itten, 2005. Towards a direct comparison of field- and laboratory goniometer measurements. Submitted to: IEEE Transactions on Geoscience and Remote Sensing